TECHNICAL REPORT
69-11-OSD

LARGE DEFLECTIONS OF AN INFLATED CYLINDRICAL TENT

by
Edward W. Ross, Jr.

July 1968

UNITED STATES ARMY
NATICK LABORATORIES
Natick, Massachusetts 01760

Office of the Scientific Director

45

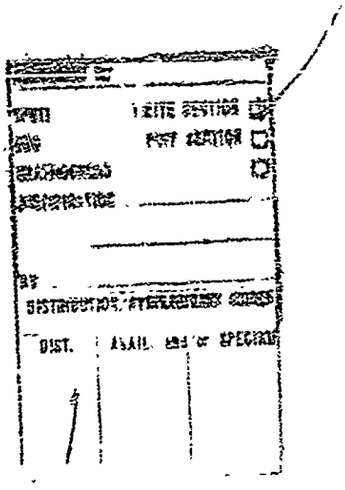

This document has been approved for public release and sale; its distribution is unlimited.

The findings in this report are not to be construed as an official Department of the Army position unless so designated by other authorized documents.

Citation of trade names in this report does not constitute an official indorsement or approval of the use of such items.

Destroy this report when no longer needed. Do not return it to the originator.

AD_____

TECHNICAL REPORT
69-11-OSD

LARGE DEFLECTIONS OF AN INFLATED CYLINDRICAL TENT

by

Edward W. Ross, Jr.

July 1968

Office of the Scientific Director
U. S. ARMY NATICK LABORATORIES
Natick, Massachusetts

FOREWORD

It has long been felt that the design of shelters could be improved by application of knowledge gained from structural mechanics methods. This paper is a significant contribution to this area and represents a first attempt to devise a realistic and usable model for simulating the behavior of an air-supported, single-wall tent. The results are in general agreement with observations of tent behavior in a wind and inspire confidence in the soundness of the approach.

TABLE OF CONTENTS

LIST OF FIGURES

ABSTRACT

This report analyzes the large deformations of a cylindrical, inflated, single-wall tent due to wind pressure and is based on the membrane theory for large deflections but small strains. The tent cross-section is a sector of a circle in the undeformed position, and the wind is blowing on it in the broadside direction. The tent motion is taken as plane, and it is assumed that the wind pressure distribution is known in the deformed state. The problem is solved by numerical analysis and results are presented for the stress, deformed shape, aerodynamic resultants and anchor forces. The problem is of theoretical interest because the linear membrane theory does not have a unique solution for it, and also because it illustrates that the method of small deformations superposed on large is of little help when the large deformation is of inextensional type.

LARGE DEFLECTIONS OF AN INFLATED CYLINDRICAL TENT

1. Introduction

In recent years the use of pressure-supported structures has become attractive to aerospace and military equipment designers. The literature dealing with these problems includes work by Leonard, Brooks and McComb [1], Stein and Hedgepeth [2] and a book by Otto [3].

The present paper describes an investigation of the deflections suffered by a pressure-supported tent when subjected to a wind. The tent has the shape of a long sector of a cylinder, held down at the edges, and the wind is in the broadside direction (i.e., parallel to the ground and perpendicular to the axis of the cylinder). A right-handed cartesian coordinate system is chosen as shown in Figure 1. If the tent is long enough it is reasonable that (except near the ends) the deformation will be in the x-y plane, possibly with a uniform z-stretch superposed.

We shall postulate that the tent material is perfectly flexible, i.e., it has zero bending stiffness. This means that it is unstable when either principal stress is negative, and we shall be concerned here only with the case where neither principal stress is negative. We assume further that the tent material is not highly elastic in tension, i.e., the strains are always small, and it is adequate to use a linear elastic law for an orthotropic material. Although the strains are small, the rotations and displacements may be large, and we shall employ large-deflection membrane theory in our analysis.

Initially, it is assumed that three kinds of loads act on the shell, external wind pressure, internal inflation pressure and gravity. If the wind is very

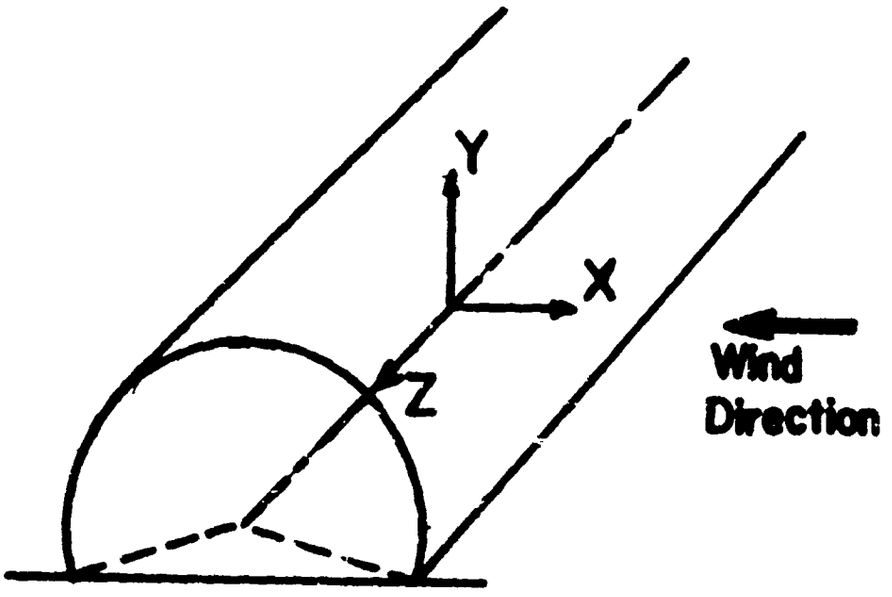

Figure 1. Orientation of Tent and Wind

weak, all these forces may be of comparable size, but, when the wind is at all strong, the pressure forces are much larger than the gravity forces, which may then be neglected.

The fundamental analysis of this problem is described in Section 2, and its final formulation as an integro-differential equation system is obtained in Section 3. A general solution in finite terms could not be obtained although a simple special case is solved in Section 3. Section 4 describes a numerical analysis of the problem which led to a computer program that produced the results described in Section 5. The paper concludes with the discussion of Section 6.

2. Analysis

We assume that the undeformed body is a portion of a cylindrical shell of constant thickness h, whose middle surface is described by cylindrical coordinates a, ϕ, Z which are related to the cartesian coordinates X, Y, Z of the undeformed shell by (see Figure 2a)

$$X = a \sin \phi, \quad Y = -a \cos \phi.$$

The cylindrical coordinates of the deformed middle surface, r, ϕ, z are related to its cartesian coordinates x, y, z by (see Figure 2b)

$$x = r \sin \phi, \quad y = -r \sin \phi.$$

The deformation is assumed to carry the initially circular cylinder into a non-circular cylinder by means of a plane motion with a superposed uniform stretch*, and is defined by

$$r = r(\phi), \quad \phi = \phi(\phi), \quad z = \lambda Z \qquad (\lambda \text{ constant}) \tag{1}$$

The mixed (i.e., physical) middle surface strain components are

$$\left.\begin{aligned} \gamma_{\phi}^{\ \phi} &= \frac{1}{2}\left[\left(\frac{d\phi}{d\phi}\right)^2\left\{\left(\frac{r}{a}\right)^2 + \left[\frac{1}{a}\frac{dr}{d\phi}\right]^2\right\} - 1\right] \equiv \gamma_s \\ \gamma_Z^{\ Z} &= \frac{1}{2}(\lambda^2 - 1) \equiv \gamma_z \\ \gamma_Z^{\ Z} &\equiv \gamma_{sz} = 0 \end{aligned}\right\} \tag{2}$$

*The possibility of this uniform stretch occurring in practice depends on the way in which the tent is held down at the edges.

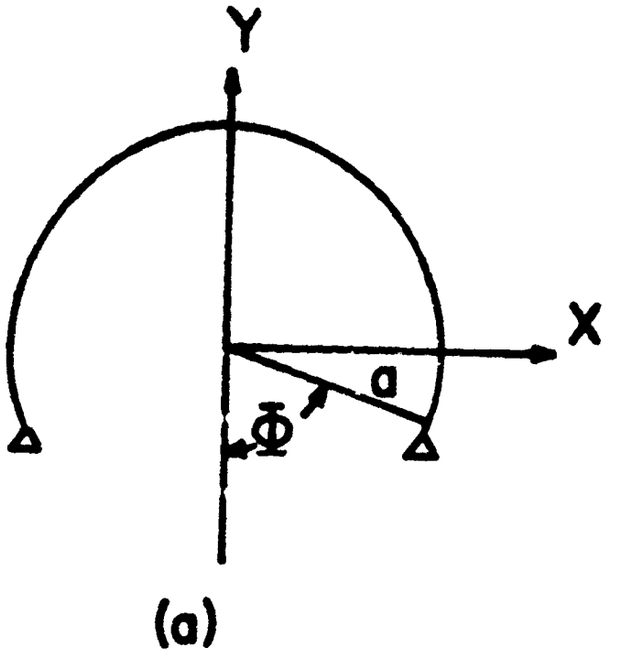

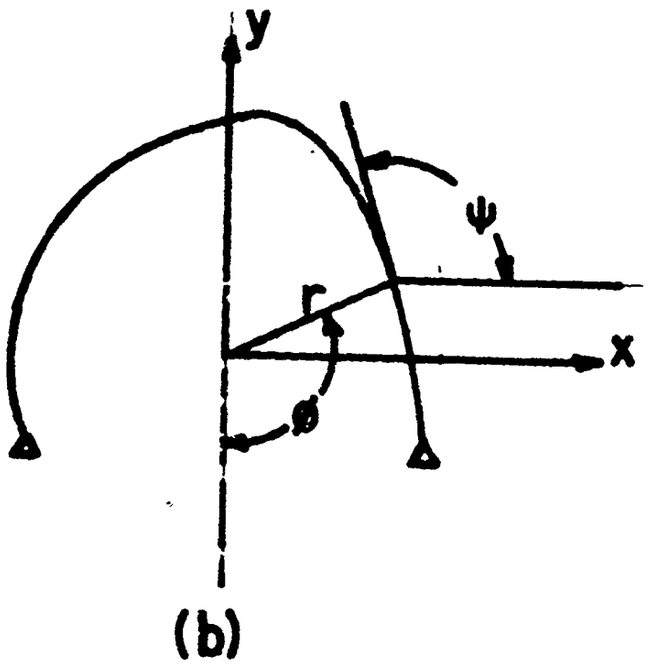

Figure 2. (a) Coordinate System in the Undeformed Tent
(b) Coordinate System in the Deformed Tent

If s is the deformed circumferential arc length and ψ is the slope angle of the deformed circumferential arc, we have by geometry (Figure 3)

$$ds/d\phi = [r^2 + (dr/d\phi)^2]^{1/2} \tag{3}$$

$$\psi = \phi - \Gamma \tag{4}$$

where

$$\Gamma = \arctan (r^{-1}\, dr/d\phi). \tag{5}$$

Also, if R_s is the radius of curvature of the deformed circumferential arc,

$$1/R_s = d\psi/ds \tag{6}$$

and

$$ds/d\phi = r \sec (\phi - \psi). \tag{7}$$

The physical stress-resultants, N_s, N_z and N_{sz} in the deformed state obey the equilibrium conditions

$$(\partial N_z/\partial z) + (\partial N_{sz}/\partial s) = 0 \tag{8}$$

$$(\partial N_{sz}/\partial z) + (\partial N_s/\partial s) = \rho g h \sin \psi(s) \tag{9}$$

$$N_s/R_s = P_i - P_w + \rho g h \cos \psi(s) \tag{10}$$

where ρg is the weight density of the shell material, P_i is the uniform internal pressure and $P_w(s)$ is the non-uniform wind pressure.

The constitutive relations are those for an orthotropic thin shell undergoing small strains,

$$N_s/h = C_1\gamma_s + C_2\gamma_z \tag{11}$$

$$N_z/h = C_2\gamma_s + C_3\gamma_z \tag{12}$$

$$N_{sz}/h = C_4\gamma_{sz} \tag{13}$$

where C_1, C_2, C_3, C_4 are elastic constants.

The edge conditions express that the tent is held down at both edges during the deformation, i.e.

$$\left.\begin{aligned} r(\phi_o) &= r(\phi_L) = a \\ \phi(\phi_o) &= \phi_o, \quad \phi(\phi_L) = \phi_L \end{aligned}\right\} \tag{14}$$

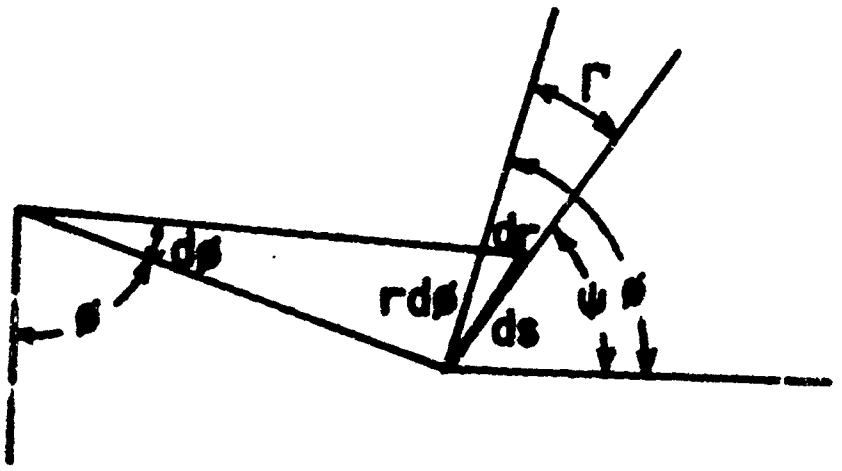

Figure 3. Geometry of the Deformed Tent

Equations (2) - (14) are the mathematical embodiment of the physical problem we wish to solve. They can be simplified slightly by using $\gamma_{sz} = 0$, whence (13) and (8) imply

$$N_{sz} = 0$$

$$N_z = N_z(s)$$

If ϕ is taken as the independent variable we may write the system as

$$dr/d\phi = r \tan(\phi-\psi) \tag{15}$$

$$d\phi/d\phi = (r/a)(1 + 2\gamma_s)^{1/2} \sec(\phi-\psi) \tag{16}$$

$$dN_s/d\phi = \rho g h r \sin\psi \sec(\phi-\psi) \tag{17}$$

$$d\psi/d\phi = (P_i - P_w + \rho g n \cos\psi)\, r \sec(\phi-\psi) / N_s \tag{18}$$

together with the constitutive relations

$$N_s/h = C_1(\gamma_2 + \nu\gamma_z), \quad N_z/h = C_1(\nu\gamma_s + \alpha\gamma_z) \tag{19}$$

and the boundary conditions (14). Here

$$\nu = C_2/C_1, \quad \alpha = C_3/C_1, \tag{20}$$

and the constant γ_z, the uniform axial strain, is taken as known. The entire system is then a fourth order, non-linear ordinary differential equation system.

We now put the equations into dimensionless form. If ρ_a and U are the mass density and free-stream velocity of the air, respectively, we set

$$\left.\begin{aligned} r &= aR, \quad N_s = hC_1 n_s, \quad N_z = hC_1 n_z \\ P_i &= q_i(1/2)\rho_a U^2, \quad P_w = q_w(1/2)\rho_a U^2 \\ \eta &= \frac{a\rho_a U^2}{2hC_1}, \quad \zeta = \frac{a\rho g}{C_1} \end{aligned}\right\} \tag{21}$$

The equations become

$$dR/d\phi = R \tan(\phi-\psi) \tag{22}$$

$$d\Phi/d\phi = R(1 + 2\gamma_s)^{-1/2} \sec(\phi-\psi) \tag{23}$$

$$dn_s/d\phi = \zeta \sin\psi \sec(\phi-\psi) \tag{24}$$

$$d\psi/d\phi = [n(q_i-q_w) + \zeta\cos\psi] R \sec(\phi-\psi)/n_s \tag{25}$$

$$n_s = \gamma_s + \nu\gamma_z, \quad n_z = \nu\gamma_s + \alpha\gamma_z \tag{26}$$

and the boundary conditions are

$$\left.\begin{aligned} R(\phi_o) &= R(\phi_L) = 1 \\ \Phi(\phi_o) &= \Phi_o, \quad \Phi(\phi_L) = \Phi_L \end{aligned}\right\} \tag{27}$$

We may identify n and ζ as dimensionless parameters measuring the ratios of pressure forces and gravity forces, respectively, to elastic forces.

3. High Wind Approximation

In a test run on a tent model in a wind tunnel [4] the numbers were

$$nC_1 = 250 \text{ lb/in.}, \qquad a = 10.5 \text{ in.}$$

$$v = 60 \text{ miles/hr} = 1056 \text{ in./sec}$$

$$\rho_a v^2/2 = .064 \text{ lb/in.}^2$$

$$\rho g h = 2.9 \times 10^{-4} \text{ lb/in.}^2$$

whence from (21)

$$\zeta = 1.2 \times 10^{-5}, \quad \eta = 2.67 \times 10^{-3}. \tag{28}$$

These values are typical of the cases where the wind is high. Since these are the most severe cases against which the tent must be designed, we shall concentrate most of our attention on them. For these cases we see that

$$\zeta << \eta << 1,$$

and therefore we may neglect the terms involving ζ in (24) and (25). We shall call this the high-wind approximation.

With this approximation (24) and (26) imply that n_s, n_ℓ, γ_s are all independent of ψ. Moreover, from (23) and (27) we obtain

$$\int_{\phi_o}^{\phi_L} (d\phi/d\phi)d\phi = (1 + 2\gamma_s)^{-1/2} \int_{\phi_o}^{\phi_L} \kappa \sec(\phi-\psi)\, d\phi$$

$$= \phi(\phi_L) - \phi(\phi_o) = \phi_L - \phi_o$$

Thus, since the strain is small, we get finally

$$\gamma_s = (\phi_L - \phi_o)^{-1} \int_{\phi_o}^{\phi_L} [R \sec(\phi - \psi) - 1]d\phi \tag{29}$$

Then the basic system reduces to

$$dR/d\phi = R \tan(\phi-\psi) \tag{30}$$

$$d\psi/d\phi = (\eta/n_s)(q_j - q_w) R \sec(\phi - \psi) \tag{31}$$

with

$$R(\phi_o) = R(\phi_L) = 1 \tag{32}$$

$$n_s = \nu\gamma_z + (\phi_L-\phi_o)^{-1}\int_{\phi_o}^{\phi_L} [R \sec(\phi-\psi) - 1]d\phi. \tag{33}$$

This is now a second-order integro-differential equation system for the functions $R(\phi)$, $\psi(\phi)$ and the constant n_s. When this system has been solved, the function $\Phi(\phi)$ can be found by quadrature,

$$\Phi = \phi_o + (1-\gamma_s)\int_{\phi_o}^{\phi} R \sec[\phi(\beta)-\psi(\beta)]d\beta. \tag{34}$$

We see from (34) that $\Phi(\phi)$, which completes the definition of the deformation, can be separated as follows

$$\Phi = \Phi_i + \Phi_s$$

where

$$\Phi_i = \phi_o + \int_{\phi_o}^{\phi} R(\beta) \sec[\phi(\beta)-\psi(\beta)]d\beta$$

$$\Phi_s = -\gamma_s \int_{\phi_o}^{\phi} R(\beta) \sec[\phi(\beta)-\psi(\beta)]d\beta.$$

Φ_i defines a deformation without strain (an inextensional deformation) and Φ_s defines the very small deformation associated with the strain.

In some cases an alternative formulation of (33) may be helpful. Since n_z is independent of ϕ, we have

$$F_z = naC_1 n_z(\phi_L-\phi_o)$$

where F_z is the total axial force. Then we may rephrase (33) in terms of F_z rather than γ_z with the aid of (26),

$$n_s = \frac{\nu F_z}{naC_1(\phi_L-\phi_o)} + \frac{(a-\nu^2)}{a(\phi_L-\phi_o)}\int_{\phi_o}^{\phi_L} [R \sec(\phi-\psi)-1]d\phi \tag{35}$$

In some practical cases information about F_z may be more readily obtainable than information about γ_z and (35) will be more convenient than (33). We

notice that the parameter α which measures the degree of fabric anisotropy, enters into the final system only through (35).

We may obtain three useful identities between the pressure distribution and the tensile forces at the edges by taking various definite integrals of the equilibrium equation (31). These identities merely represent the conditions of overall equilibrium of forces and moments. To find the first two we multiply (31) by cos ψ and sin ψ, respectively, and integrate from ϕ_o to ϕ_L, obtaining

$$n_s(\sin \psi_L - \sin \psi_o) = n\int_{\phi_o}^{\phi_L} (q_i - q_w) R \cos \psi \sec (\phi - \psi) d\phi \qquad (36)$$

$$n_s(\cos \psi_o - \cos \psi_L) = n\int_{\phi_o}^{\phi_L} (q_i - q_w) R \sin \psi \sec (\phi - \psi) d\phi \qquad (37)$$

The third identity is found as follows: Multiply (31) by R sin $(\phi - \psi)$ and integrate from ϕ_o to ϕ_L,

$$n_s\int_{\phi_o}^{\phi_L} R(d\psi/d\phi) \sin (\phi - \psi) d\phi = n\int_{\phi_o}^{\phi_L} (q_i - q_e) R^2 \tan (\phi - \psi) d\phi$$

We have

$$R(d\psi/d\phi) \sin (\phi - \psi) = d[R \cos (\phi - \psi)]/d\phi - \cos (\phi - \psi)\left[dR/d\phi - R \tan (\phi - \psi)\right]$$

The last term vanishes because of (30), and so we obtain

$$n_s[\cos (\phi_L - \psi_L) - \cos (\phi_o - \psi_o)] = n\int_{\phi_o}^{\phi_L} (q_i - q_e) R^2 \tan(\phi - \psi) d\phi \qquad (38)$$

We may express the horizontal and vertical force resultants and the overturning moment resultants (see Figure 4) due to the wind pressure and inflation

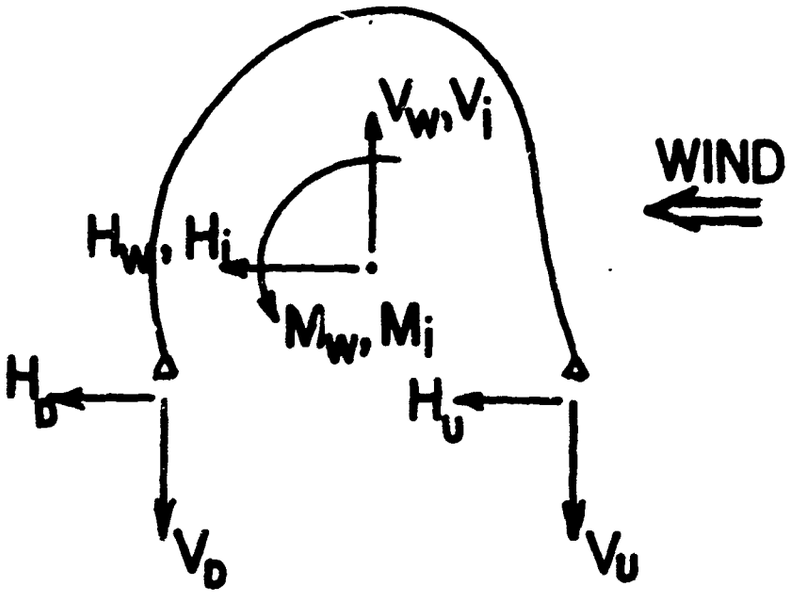

Figure 4. Sign Conventions for Pressure Force and Moment Resultants

pressure on the deformed tent at

$$\begin{bmatrix} V_w \\ H_w \end{bmatrix} = \int_{\phi_o}^{\phi_L} R\, q_w \begin{bmatrix} \cos\psi \\ \sin\psi \end{bmatrix} \sec(\phi - \psi)\, d\phi \tag{39}$$

$$\begin{bmatrix} V_i \\ H_i \end{bmatrix} = -\int_{\phi_o}^{\phi_L} R\, q_i \begin{bmatrix} \cos\psi \\ \sin\psi \end{bmatrix} \sec(\phi - \psi)\, d\phi \tag{40}$$

$$M_w = \int_{\phi_o}^{\phi_L} R^2\, q_w \tan(\phi - \psi)\, d\phi \tag{41}$$

$$M_i = -\int_{\phi_o}^{\phi_L} R^2\, q_i \tan(\phi - \psi)\, d\phi \tag{42}$$

Further, the vertical and horizontal components of the restraining forces at the upwind edge, ϕ_o, and the downwind edge, ϕ_L, are respectively

$$V_u = n_s \sin\psi_o,\ V_D = n_s \sin(2\pi - \psi_L) = -n_s \sin\psi_L \tag{43}$$

$$H_u = -n_s \cos\psi_o,\ H_D = n_s \cos(2\pi - \psi_L) = n_s \cos\psi_L \tag{44}$$

Then the relations(36) - (38) may be written

$$V_u + V_D = n\,(V_i + V_w) \tag{45}$$

$$H_u + H_D = n\,(H_i + H_w) \tag{46}$$

$$V_u \sin\phi_o + V_D \sin\phi_L - H_u \cos\phi_o - H_D \cos\phi_L = n\,(M_w + M_i) \tag{47}$$

These definitions are useful in describing the forces acting on the tent during its deformation.

The system (30), (31) can be written in the form of a single, second-order differential equation by solving (31) for R and inserting the result in (30). We get

$$d^2(\sin\Gamma)/d\phi^2 - G\, d(\sin\Gamma)/d\phi + \sin\Gamma = \cos\Gamma. \tag{48}$$

where

$$G = G(\phi) = d[\log(q_i - q_w)]/d\phi, \tag{49}$$

and R can be found from

$$R = [\cos\Gamma + d(\sin\Gamma)/d\phi]\, n_s/[n(q_i - q_w)]. \tag{50}$$

Equation (48) is still in general non-linear and is awkward because of the singularity where $q_i = q_w$, see (49). For purposes of numerical analysis the system (30), (31) is more convenient. However, (48) - (50) is useful for finding approximate solutions in certain special cases.

First, if the total pressure, $q_i - q_w$, is constant, then $G = 0$, and (48) can be solved very easily. Some complications still remain due to the non-linearity of (50). If, in addition, $\sin\Gamma$ is small enough so that $\cos\Gamma = 1$, the system can easily be solved for R and $\sin\Gamma$, and the results inserted in (33) or (35) to evaluate n_s. Some care is required in these manipulations, but for the case

$$\phi_L = 2\pi - \phi_o,\ \Gamma_z = 0,\ \alpha = 1$$

we obtain, using (35), the results

$$
\left.
\begin{aligned}
R &= 1 + C\,(\cos\phi_o - \cos\phi) \\
\sin\Gamma &= -\,C \sin\phi \\
n_s &= \frac{n\,(q_i - q_w)}{1 - C\cos\phi_o} \\
C &= \frac{n\,(\pi - \phi_o)(q_i - q_w)}{(1 - \nu^2)\,[(\pi - \phi_o)\cos\phi_o + \sin\phi_o]}
\end{aligned}
\right\} \qquad (51)
$$

Apart from this simple solution, the integro-differential equation systems (30) - (32) and (33) or (35) seem intractable to purely analytical methods, and recourse was had to numerical analysis at this point.

4. Numerical Analysis

The computer program for solving the systems (30) - (32) and (35) is based on the following procedure, assuming that we know the function $q_w(\phi)$ and the constants ϕ_o, ϕ_L, n, q_i, v, Γ_z and α. A trial value is chosen for n_s. The second-order differential equation system (30) - (32) is solved, using the trial value of n_s. The solutions for $R(\phi)$ and $\psi(\phi)$ are then substituted into either (33) or (35) and a new value of n_s is obtained, which is compared with the trial value. If the two do not agree, a new trial value is used and the procedure repeated until agreement is obtained. When agreement has been reached, the function $\Phi(\phi)$ is found by a numerical integration and various quantities of physical interest, V_i, V_w, H_i, H_w, M_i, M_w, V_u, V_D, H_u and H_D are also calculated.

The boundary value problem posed by the differential equation system (30) - (32) was solved by repeated use of the second-order Runge-Kutta procedure for a pair of first-order equations, as described, for example in [5]. A trial-and-error procedure was needed because the boundary conditions were of two-point type. Various values were tried for $\psi(\phi_o)$ until one was obtained that generated a solution having $R(\phi_L) = 1$. This process was systematized by use of an iterative procedure to produce rapid (but not sure) convergence to the solution having $R(\phi_L) = 1$.

The accuracy of the program was tested in various ways. For a uniform pressure distribution, numerical results were compared with (51) and gave satisfactory agreement, but this was not a severe test of the computation scheme. A more stringent procedure was to make successive refinements of the mesh for a pressure distribution typical of a broadside wind on the tent. Since $|n_s| \ll 1$, and n_s is obtained in (33) by integrating quantities, R and ψ, that are not small, a good

deal of cancellation takes place in calculating n_s. This suggests that the stability of n_s is a sensitive test of the accuracy of the entire computation. Several such tests were made. For example, using the values

$$\phi_o = 60^o, \quad \phi_L = 2\pi - \phi_o = 300^o, \quad \eta = .267 \times 10^{-2}$$

$$\alpha = 1, \quad \nu = .3, \quad q_i = .5$$

and taking for $q_w(\phi)$ a distribution typical of a broadside wind, the following results were obtained from calculations with K mesh points

K	n_s
24	.002776
48	.002749
96	.002742

The value of n_s is quite stable in this example, and several similar tests gave like results.

In general, the program worked well although poor initial guesses for $\psi(\phi_o)$ or n_s sometimes caused it to fail. This difficulty could be evaded by changing the initial guesses. A different stumbling block is encountered when $\psi - \phi = \pi/2$ at some point. At these points there is a singularity in the differential equation system (30) and (31), which is caused by the use of ϕ as independent variable (see (7)). If this singularity is to occur, the deflections must be very large, far larger than could be tolerated in use. This singularity did occur in some extreme cases among the calculations described in the next Section.

5. Results for Several Cases

The program was used to calculate deflections, strains and other quantities of physical interest for a cylindrical tent with parameters as given in (28). The values $\nu = .3$, $F_z = 0$ (no net longitudinal force) and $\alpha = 1$ (isotropic tent material) were used.

Two different functions were used for the wind pressure distribution $q_w(\phi)$. The main one (see Figure 5), called (I), was determined by making pressure measurements around the tent during wind tunnel tests. It is important to notice that the wind tunnel tests were conducted with rather high inflation pressures, q_i, so that the deformations were fairly small. Since the wind pressure distribution depends on the deformed shape (i.e., there is coupling between the fluid flow problem and the elastic deformation problem), this wind pressure distribution may not be an accurate approximation to the true one when the inflation pressure is low.

The second wind pressure distribution, designated as (II), is a discontinuous, purely hypothetical one, given by

$$\begin{aligned} q_w &= .8 \qquad 60^\circ \leq \phi < 150^\circ \\ q_w &= -.8 \qquad 300^\circ \geq \phi > 150^\circ. \end{aligned} \tag{52}$$

Although this has the same general shape as the experimental wind pressure distribution, it is very different in detail, and there is no reason to expect the results to be similar.

All these calculations were carried out with 96 mesh points, for a range of q_i

$$\begin{aligned} 0 \leq q_i \leq 2.5 \quad &\text{for (I)} \\ .3 \leq q_i \leq 2.5 \quad &\text{for (II)} \end{aligned}$$

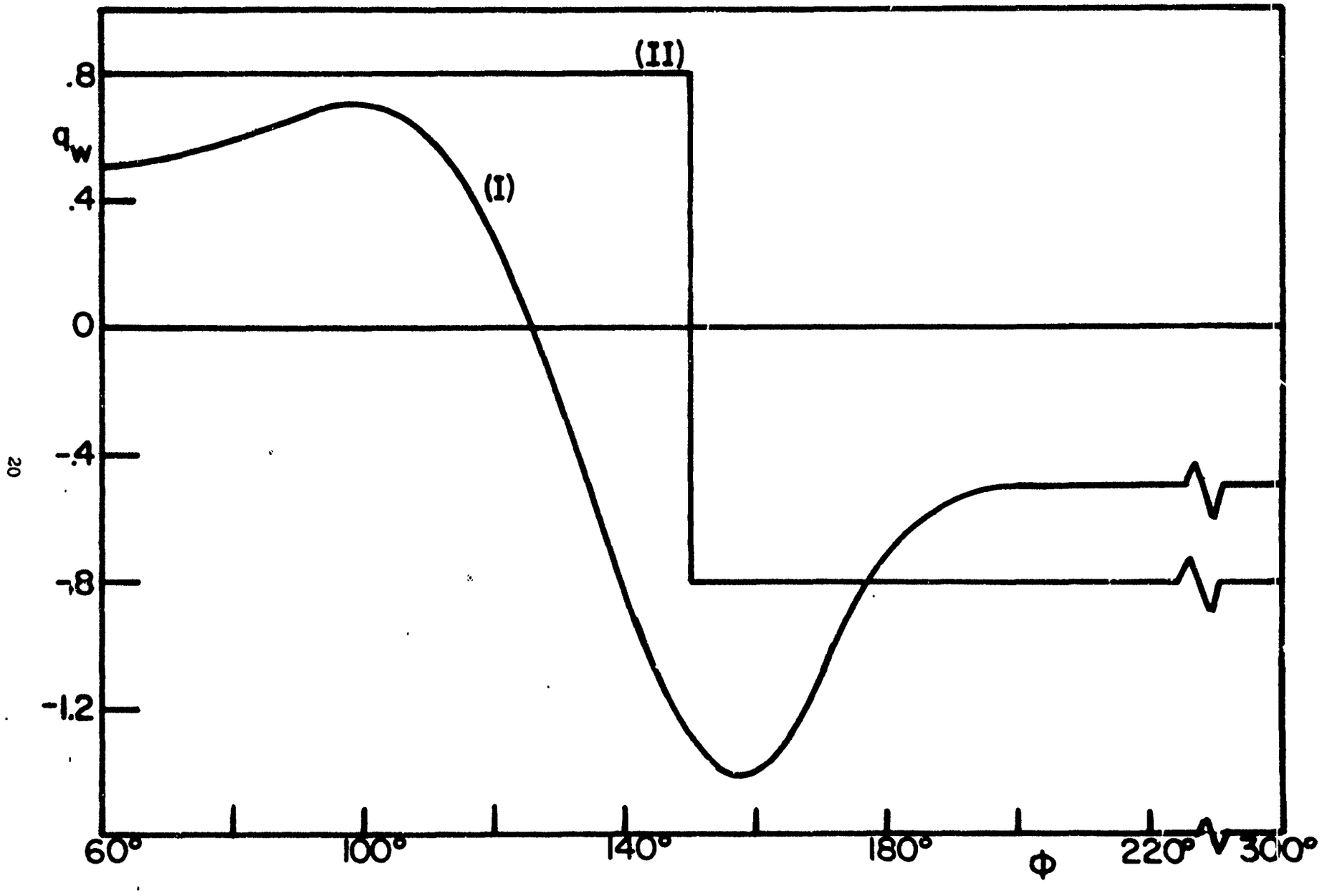

Figure 5. Two Pressure Distributions Assumed in the Calculations

When the distribution (II) was tried for $0 \leq q_i < .3$, the calculation could not be completed owing to the fact that $\psi - \gamma$ took the value $\pi/2$ at some points. The results of the calculations that were completed are shown in Figures 6 - 11 as graphs of various parameters plotted against q_i. Since the maximum deformation magnitude decreases when q_i increases, we may regard q_i as an inverse measure of the magnitude of deformation. When $q_i >> \max q(\phi)$, the results should agree with the constant pressure, small deflection results (51).

We see from Figure 6 that the tensile stress, n_s, is almost linearly dependent on q_i and is not affected much by the change in pressure distributions. The edge angle on the upwind side, $\psi(\phi_c)$, decreases non-linearly as q_i increases, especially when q_i is small. Also, it is greater for Distribution (II) than for (I). The wind resultants, V_w, H_w and M_w, which are shown in Figure 7, are sensitive to changes in the wind pressure distribution (i.e., the results for (I) and (II) differ substantially) but not especially so to changes in q_i. The vertical resultant of the inflation pressure, V_i, is also graphed in Figure 7 and increases linearly with q_i, being scarcely affected by the wind distribution. H_i and M_i are negligible compared with H_w and M_w and are not shown.

The deformed tent radii, $R(\phi)$, for the two wind distributions are plotted in Figures 8 and 9. Also, the actual deformed shapes in several different cases are displayed in Figure 10.

For the discontinuous pressure distribution, (II), it is easy to derive certain conclusions that serve as partial checks on the computed results. First, for

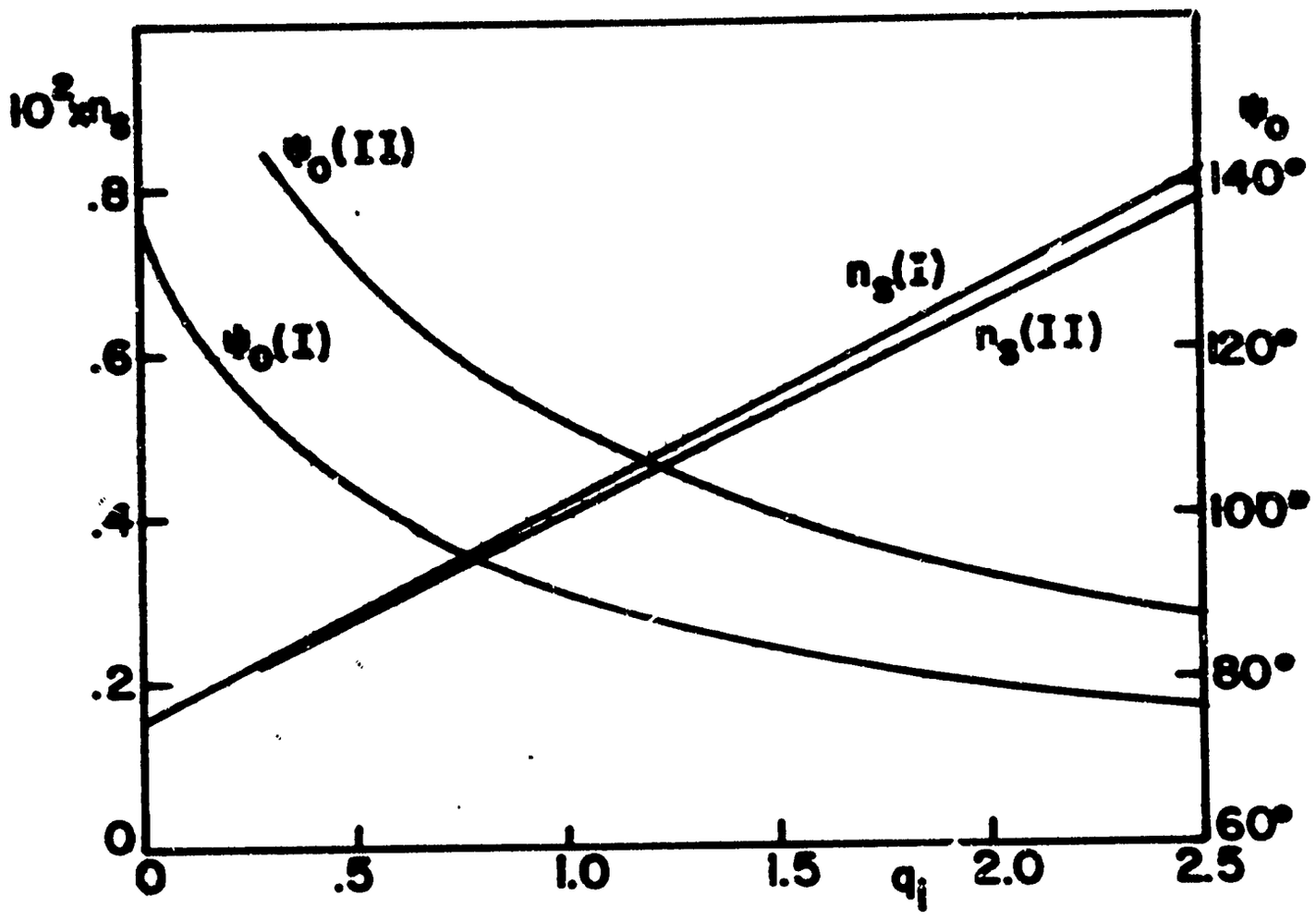

Figure 6. Tensile Stress n_s, and Upwind Edge Angle, ψ_o, for Wind Pressure Distribution (I) and (II) as Functions of q_i

small deformations

$$\psi = \phi, \quad R = 1$$

we may obtain the wind pressure resultants by inserting the pressure distribution (II), given by (52), into (39) and (41). We obtain

$$V_w = .8, \quad H_w = .8(1 + \sqrt{3}) = 2.185, \quad M_w = 0 \tag{53}$$

Second, the inflation pressure resultants are found similarly to be

$$V_i = 2q_i \sin \phi_o = \sqrt{3}\, q_i \tag{54}$$

$$h_i = M_i = 0.$$

Figure 7 shows that the small-deflection estimate (54) for V_i remains very accurate even for large deflections (i.e., small q_i). As far as can be determined from Figure 7, $V_w(II)$, $H_w(II)$ and $M_w(II)$ all approach the limiting values given by (53) as q_i becomes large. Finally, we know from (10) that the deformed shape of the tent is made up of two arcs of circles joined smoothly at the ray $\phi = 150^\circ$ and passing through the points $R = 1$ at $\phi = 60^\circ$ and 300°. The shape shown in Figure 10 is seen to have this property with good accuracy.

The edge-restraint forces, from which the ground anchor forces can be estimated, are shown in Figures 11 and 12. These forces should be related to the tent resultants by (45) - (47), and it can be seen that this is true with good accuracy. For example, for the distribution (II) and $q_i = .3$ (which is an extreme case) we have

$$V_u = .1337, \quad V_D = .1010, \quad H_u = .1841, \quad H_D = .2038$$

$$V_i = .4630, \quad V_w = .3707, \quad h_i = .002, \quad h_w = 1.436,$$

$$M_i = -.302, \quad M_w = -.6260$$

and therefore

$$V_u + V_D = .235, \qquad n(V_i + V_w) = .222$$

$$H_u + H_D = .388, \qquad n(H_i + H_i) = .383$$

$$V_u \sin \phi_o + V_D \sin \phi_L - H_u \cos \phi_o - H_D \cos \phi_L = -.168$$

$$n(Mw + Mi) = -.167$$

We conclude that the program is sufficiently accurate for engineering purposes.

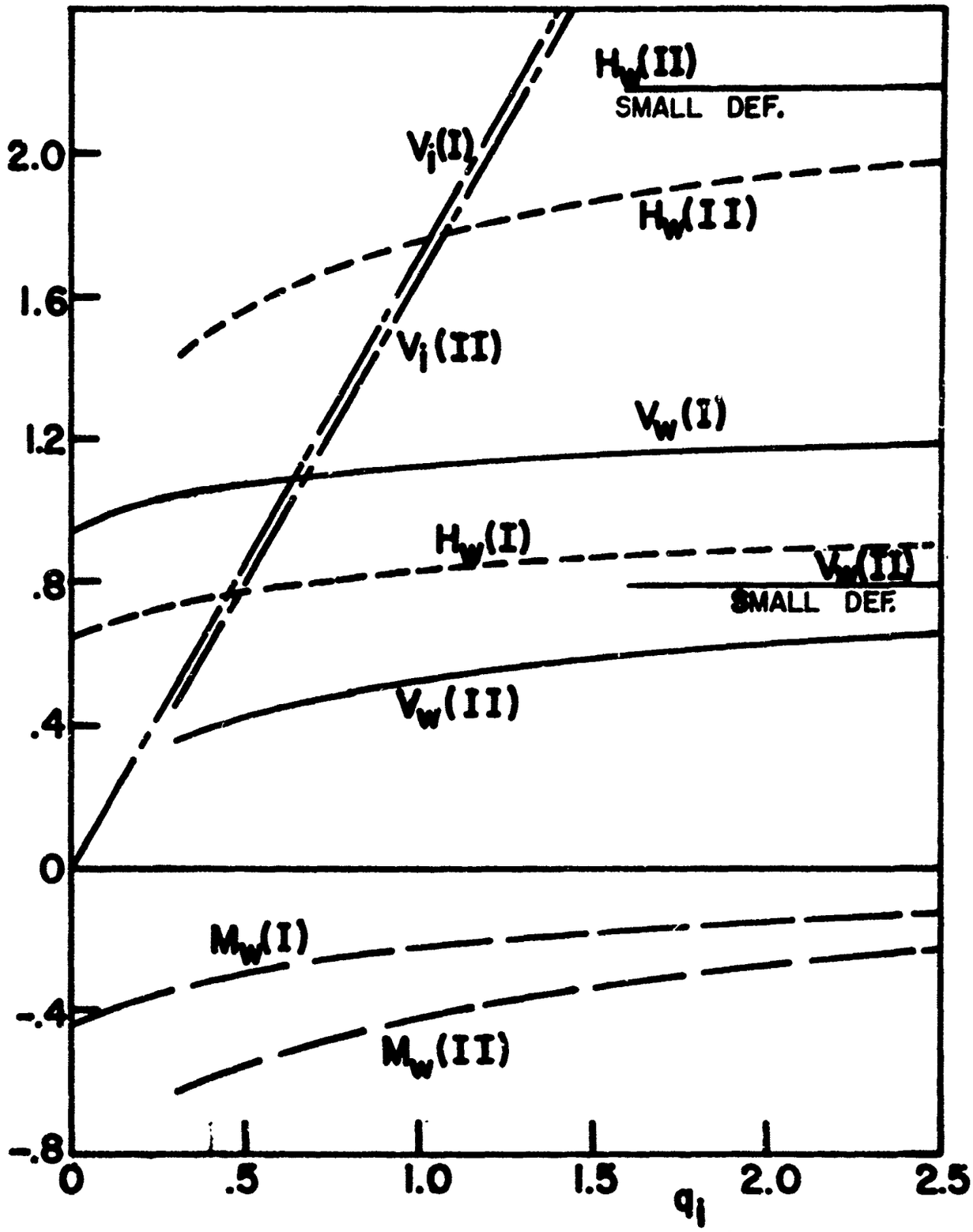

Figure 7. Wind Force and Moment Resultants and Vertical Inflation Force as Functions of q_i

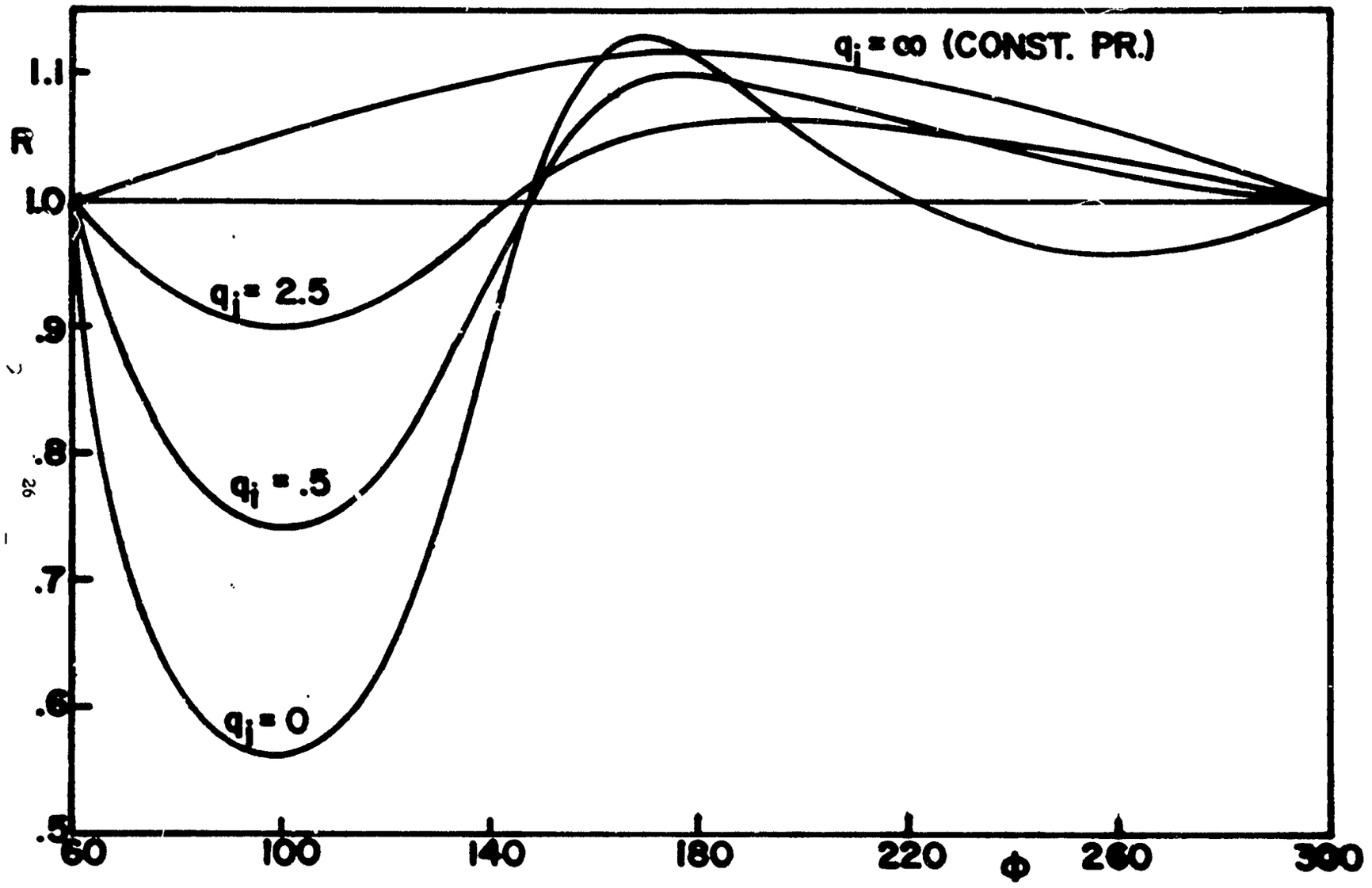

Figure 8. Deformed Tent Radius, R, as a Function of ϕ for Wind Pressure Distribution (I) and Various Inflation Pressures, q_i

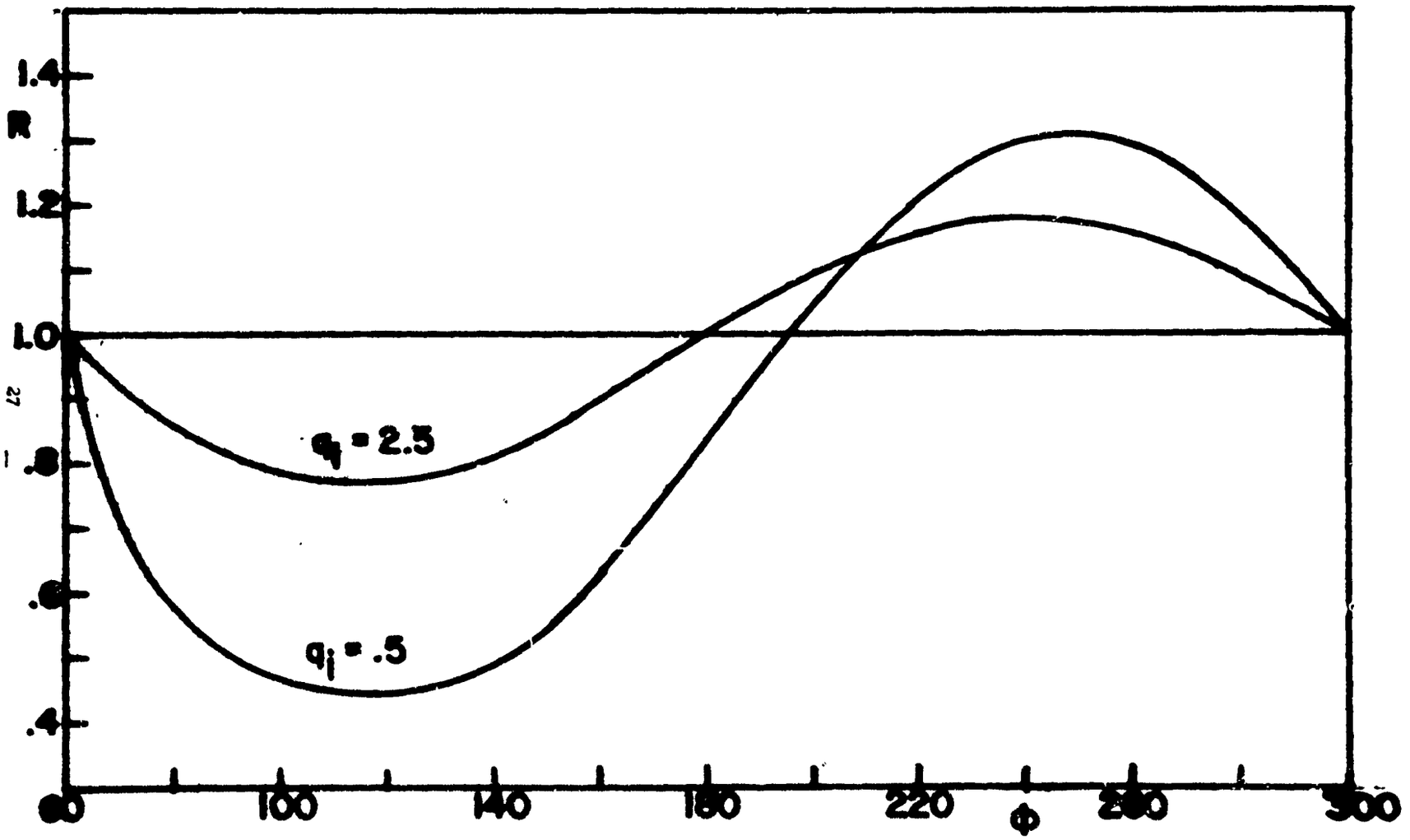

Figure 9. Deformed Tent Radius, R, as a Function of ϕ for Discontinuous Wind Pressure Distribution (II) and Two Inflation Pressures, q_i

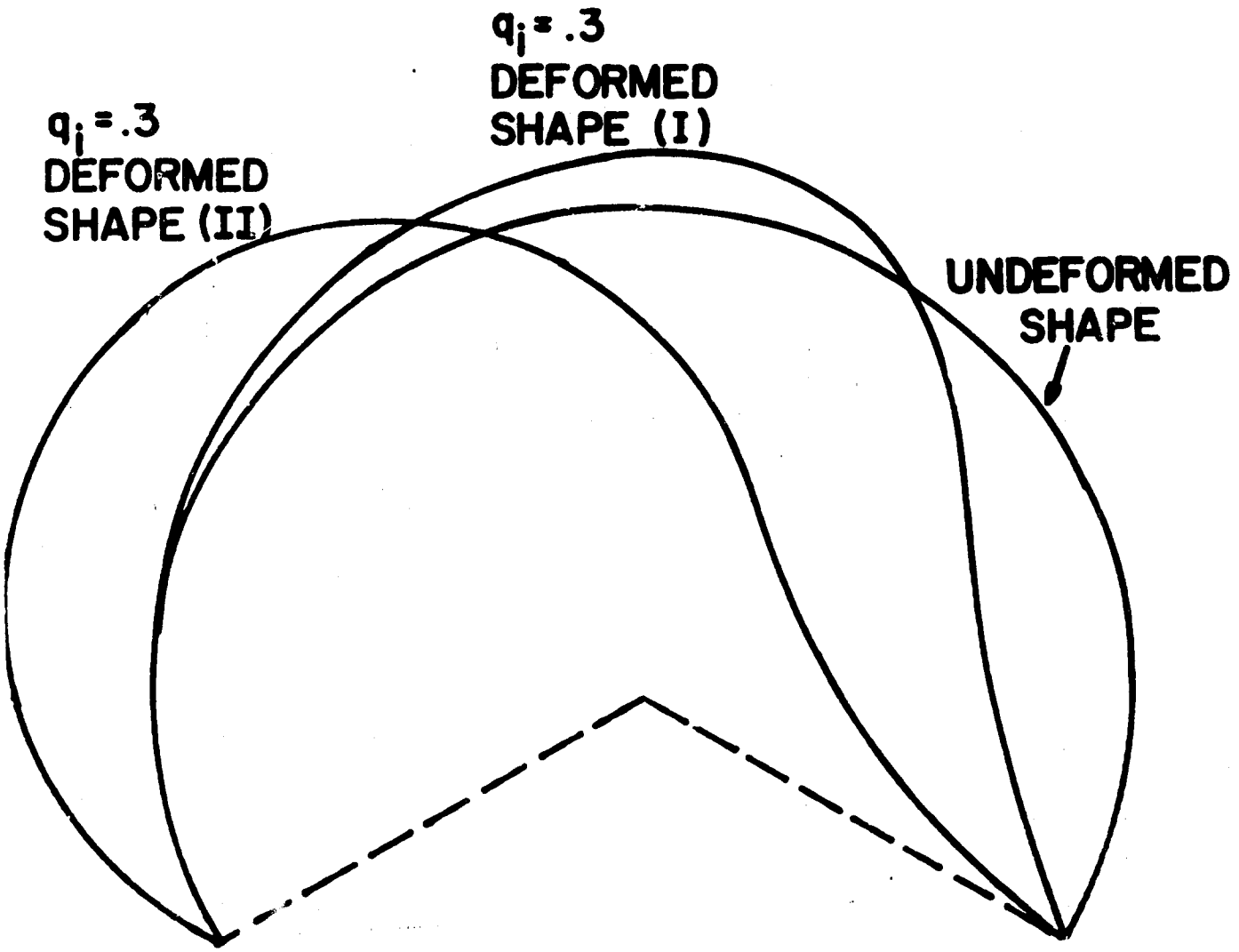

Figure 10. Deformed Shapes for the Two Wind Pressure Distributions and Inflation Pressure $q_i = .3$

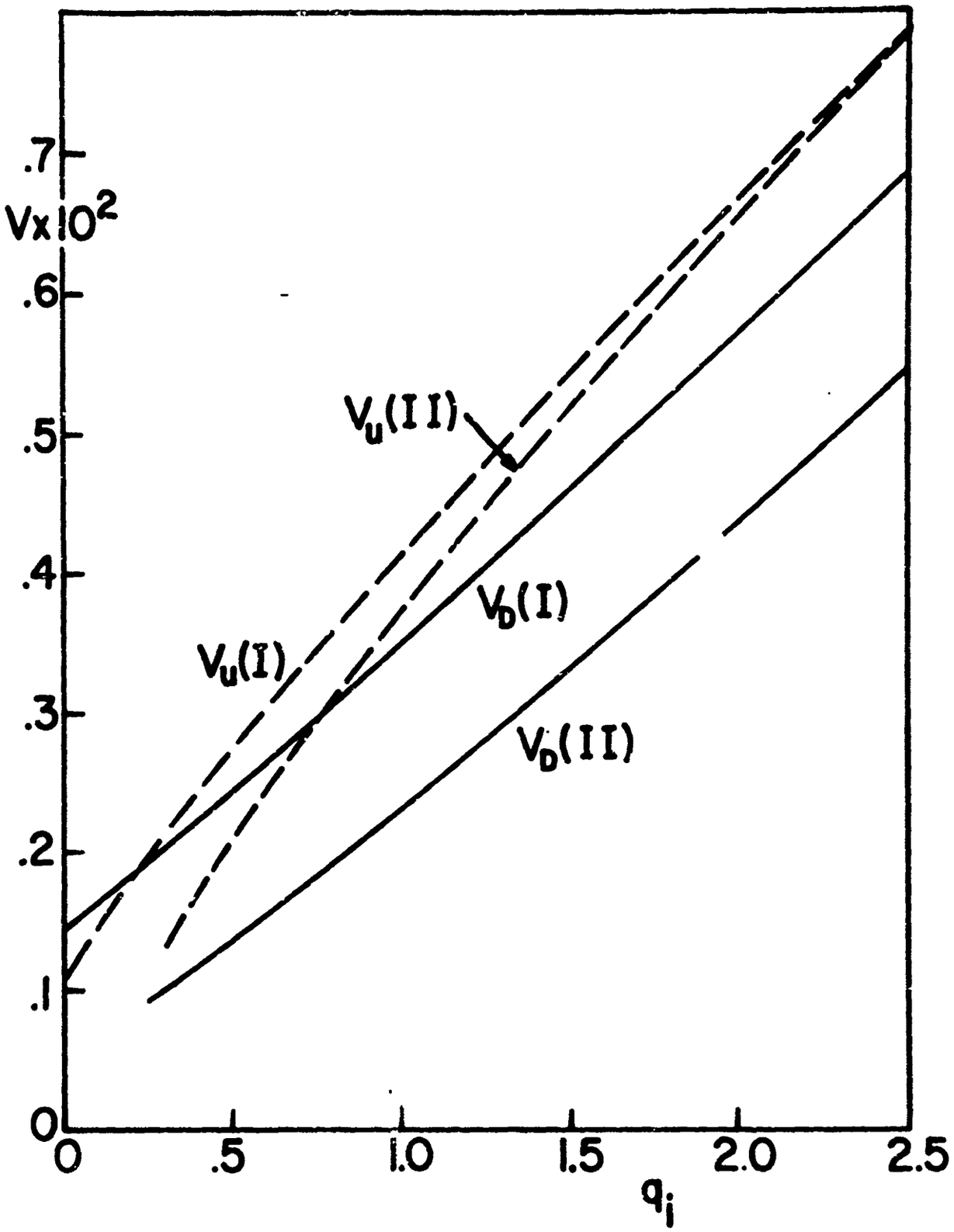

Figure 11. Vertical Components of Edge Restraint (Ground Anchor) Forces as Functions of q_i for the Two Wind Pressure Distributions

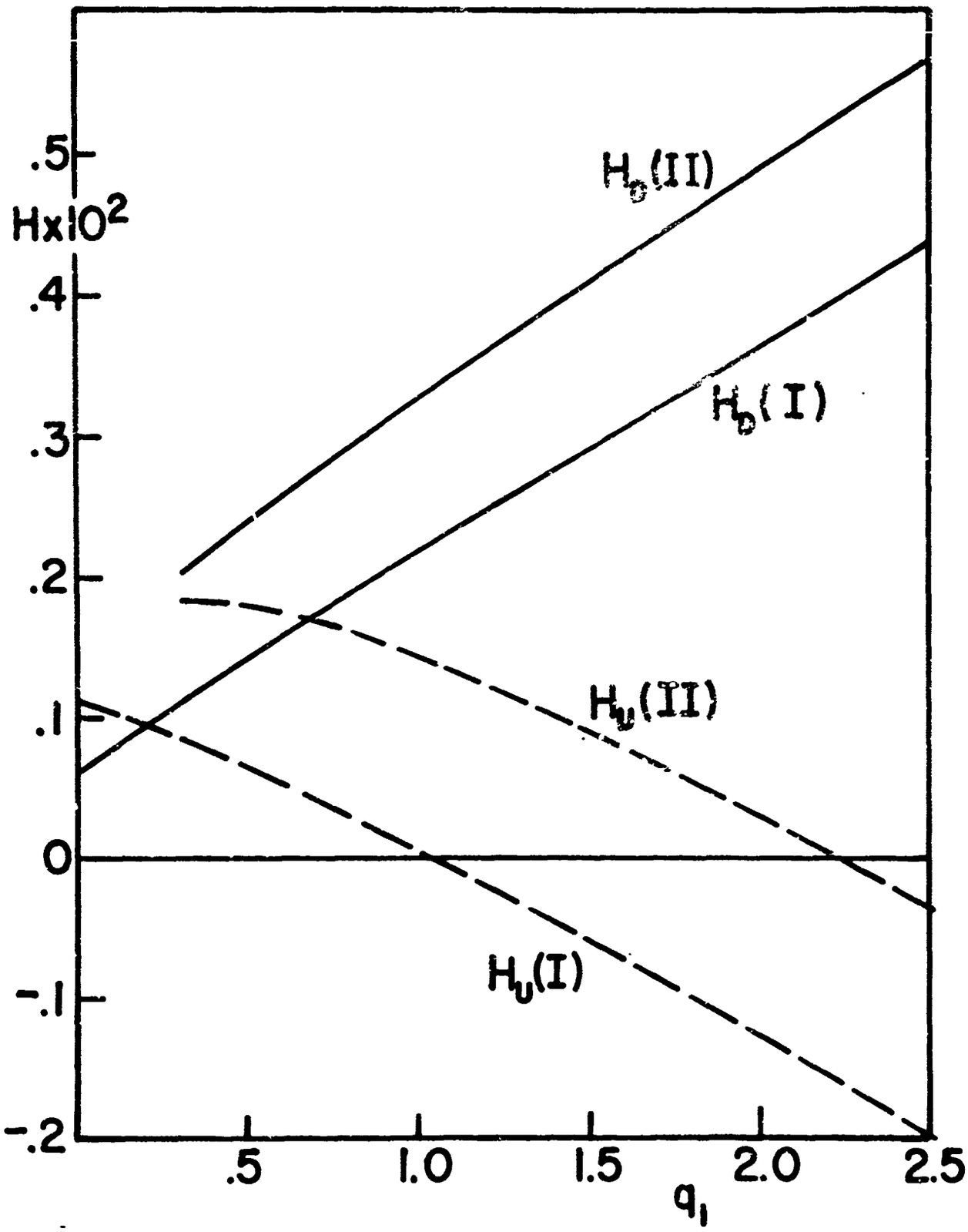

Figure 12 Horizontal Components of Edge Restraint (Ground Anchor) Forces as Functions of q_i for the Two Wind Pressure Distributions

6. Discussion

There are several aspects of this problem that are worth further discussion.

First, it is important to understand what has been done in this analysis and how it is related to the practical problem of predicting tent behavior. The central point is that we have taken the wind-pressure in the deformed state as known. From it we have calculated the deformed shape, under the kinematic assumptions (1). In attempting to use these results in practice, we face the obstacle of not knowing the wind-pressure distribution in the deformed state. To analyze the problem completely, we need to know the wind pressure distribution for every reasonable deformed state (in this connection see the comments of Truesdell and Noll [6]), a severe requirement in view of the fact that turbulent separation occurs for most tent shapes. Moreover, experiments [4] show that at sufficiently low inflation pressures the tent executes a large lateral vibration. To analyze these cases we must also consider inertia forces in the tent and possibly also in the fluid. From these remarks it should be clear that, while this paper presents necessary and useful information about tent deformation, a great deal remains to be done before a practically satisfactory prediction of tent behavior is possible.

Second, it is necessary to be careful about our interpretation of the small deflection results in this problem. We assume that the tent is in the undeformed state, with circular cylindrical shape, in the complete absence of gravity and pressure forces. If gravity alone acts, the tent will, of course, collapse immediately, and the analysis of the system (22) - (27) with $\eta = 0$ and $\zeta > 0$ would show this by predicting $n_s < 0$ for some portion of the shell. If

gravity and inflation pressure are both operative, but there is no wind, then the tent will undergo only small deflections from its undeformed shape, provided the inflation pressure, nq_i, is above a certain minimum value, such that $n_s > 0$ everywhere. We may denote this deformed state, which the tent assumes in calm air, by DSC. Now, when a high wind is turned on, the tent undergoes such large deformations that the deformations associated with DSC are negligible by comparison, as are the gravity forces. This is the basis on which the system (30) - (33) was derived. When we now make a small deflection analysis of this system to get (51), we must remember that gravity forces have been neglected. The actual deformations that occur, when the wind and inflation pressures are very low, are not accurately given by (51), and as the wind velocity approaches zero, (51) does not approach the solution DSC.

The remaining comments have to do with the relation between this problem and the general theory of thin shells.

It is interesting that the linear membrane theory version of this problem does not have a unique solution for the displacements because the edge fixity implies conditions of vanishing normal displacement. Such conditions lead to non-uniqueness within linear membrane theory (see Novozhilov [7]). Thus, although the stress, n_s, given by (51), agrees as $\eta \to 0$ with the stress obtained from linear membrane theory, there is no unique, linear solution with which to compare the deflections of (51).

The similarity of this problem to that for curved rods might lead us to expect that a theory for plane, initially curved rods, similar to the one given in Love [6], would be useful here. Such is not the case, for in that theory the rods are assumed to deform without extension while the extension plays an

important part in the analysis of this problem. We have already pointed out that the complete motion consists of a small extensional deformation together with a possibly large inextensional deformation. Although the extensional deformation is small, it is absolutely crucial because it determines the stress through the constitutive relation.

Finally, one might also hope to treat the problem by means of the theory of small deformations superposed on large, as described by Green, Rivlin and Shield [9], Green and Zerna [10], or for elastic membranes, Shield and Corneliussen [11]. The natural procedure here consists of trying to find the large inextensional deformation first and then superposing the small extensional deformation. This does not work because the theory supposes that the stresses associated with the small deformation are small compared with the stresses of the large deformation, while exactly the opposite is the case here. Another way of looking at it is that in this theory we imagine the large deformation as determined by conditions of equilibrium with the initially applied loads, and the theory fails because the large inextensional deformation causes no stresses and therefore cannot be in equilibrium with any applied loads. In fact the large, inextensional deformation is determined by its interaction with the small extensional deformation, and the two cannot be found separately.

7. References

1. R. W. Leonard, G. W. Brooks, H. G. McComb, Jr., "Structural Considerations of Inflatable Re-entry Vehicles," NASA TN D-457, Langley Research Center (Sep 1960).

2. M. Stein and J. M. Hedgepeth, "Analysis of Partly Wrinkled Membranes," NASA TN D-813, Langley Research Center (July 1961).

3. F. Otto, "Tensile Structures," MIT Press, Cambridge, Mass. (1967).

4. J. Bicknell and R. Yegnayan, "Wind Tunnel Tests on an Air Supported Tent Model," MIT Wright Brothers Wind Tunnel Report No. 1024 to U. S. Army QMR&E Command, Natick, Mass. (June 1963).

5. M. Abramowitz and I. A. Stegun, "Handbook of Mathematical Functions," National Bureau of Standards, App. Math. Series 55 (1964), p. 897.

6. C. Truesdell & W. Noll, "Non-linear Field Theories of Mechanics," Encyclopedia of Physics, Vol III/3. Berlin, Springer-Verlag (1965).

7. V. V. Novozhilov, "The Theory of Thin Shells," Groningen, The Netherlands, P. Noordhoff Ltd. (1959), pp. 97-99.

8. A. E. H. Love, "The Mathematical Theory of Elasticity," New York, Dover Publications, 4th ed. (1944), Chap. 18-21.

9. A. E. Green, R. S. Rivlin and R. T. Shield," General Theory of Small Elastic Deformations Superposed on Finite Elastic Deformations," Proc. Roy. Soc. A Vol. 211 (1952), pp. 128-154.

10. A. E. Green and W. Zerna, "Theoretical Elasticity," Oxford, Oxford University Press (1954).

11. A. H. Corneliussen & R. T. Shield, "Finite Deformation of Elastic Membranes with Application to the Stability of an Inflated and Extended Tube," Arch. Rat. Mech. & Anal., Vol. 7 (1961), pp. 273-304.

6. Appendix: Nomenclature

a	Undeformed tent radius (in.)
C	Constant, occurring in (51)
C_j	$j = 1, 2, 3, 4$, elastic constants (lb/in.^{2})
F_z	Total axis force (lb) on tent
H_w, H_i	Dimensionless horizontal forces on deformed tent due to wind and inflation pressures, respectively
H_u, H_D	Dimensionless horizontal restraint forces at upwind and downwind edges of tent, respectively
h	Thickness of tent fabric (in.)
N	Number of mesh points used in numerical integration
M_w, M_i	Dimensionless moment of the deformed tent, about the axis, due to wind and inflation pressures, respectively
N_s, N_z, N_{sz}	Physical stress resultants in fabric (lb/in.)
n_s, n_z	Dimensionless physical stress resultants in tangential and axial directions, respectively, see (21)
P_i, P_w	Pressure due to inflation and wind (lb/in.^{2})
q_i, q_w	Dimensionless inflation and wind pressure, see (21)
R	Dimensionless radius of deformed tent, see (21)
r	Radius of deformed tent (in.)
R_s	Radius of curvature of deformed tent (in.), see (6)
s	Deformed circumferential arc length (in.)
U	Free stream wind velocity (in./sec)
V_w, V_i	Dimensionless vertical forces on deformed tent due to wind and inflation pressures, respectively

V_U, V_D Dimensionless vertical restraint forces at upwind and downwind edges of tent, respectively

X, Y, Z Cartesian coordinates of undeformed tent

x, y, z Cartesian coordinates of deformed tent

α Dimensionless measure of degree of anisotropy, see (20)

Γ Angle in deformed state, see (4), (5)

$\gamma_\Phi^\Phi = \gamma_S$, $\gamma_Z^Z = \gamma_Z$, $\gamma_Z^\Phi = \gamma_{SZ}$ Dimensionless physical strain components, see (2)

ζ Dimensionless parameter measuring ratio of gravity forces to elastic forces

η Dimensionless parameter measuring ratio of pressure forces to elastic forces

ν Poisson Ratio

ρ_a Mass density of air (lb - $sec^2/in.^4$)

ρ_g Weight density of tent fabric ($lb/in.^3$)

Φ Cylindrical angle in undeformed tent

φ Cylindrical angle in deformed tent

φ_O, φ_L Cylindrical angles at upwind and downwind edges of tent, respectively

ψ Slope angle of deformed tent

Unclassified

Security Classification

DOCUMENT CONTROL DATA - R & D

(Security classification of title, body of abstract and indexing annotation must be entered when the overall report is classified)

1 ORIGINATING ACTIVITY (Corporate author) US Army Natick Laboratories Natick, Massachusetts 01760	2a. REPORT SECURITY CLASSIFICATION Unclassified 2b. GROUP

3 REPORT TITLE

LARGE DEFLECTIONS OF AN INFLATED CYLINDRICAL TENT

4 DESCRIPTIVE NOTES (Type of report and inclusive dates)

5. AUTHOR(S) (First name, middle initial, last name)

Edward W. Ross, Jr.

6 REPORT DATE July 1968	7a. TOTAL NO OF PAGES 36	7b. NO. OF REFS 11
8a. CONTRACT OR GRANT NO b. PROJECT NO c. d.	9a. ORIGINATOR'S REPORT NUMBER(S) 69-11-OSD 9b. OTHER REPORT NO(S) (Any other numbers that may be assigned this report)	

10 DISTRIBUTION STATEMENT

This document has been approved for public release and sale; its distribution is unlimited.

11 SUPPLEMENTARY NOTES	12 SPONSORING MILITARY ACTIVITY US Army Natick Laboratories Natick, Massachusetts 01760

13. ABSTRACT

This report analyzes the large deformations of a cylindrical, inflated, single-wall tent due to wind pressure and is based on the membrane theory for large deflections but small strains. The tent cross-section is a sector of a circle in the undeformed position, and the wind is blowing on it in the broadside direction. The tent motion is taken as plane, and it is assumed that the wind pressure distribution is known in the deformed state. The problem is solved by numerical analysis and results are presented for the stress, deformed shape, aerodynamic resultants and anchor forces. The problem is of theoretical interest because the linear membrane theory does not have a unique solution for it, and also because it illustrates that the method of small deformations superposed on large is of little help when the large deformation is of unextensional type.

DD FORM 1 NOV 68 1473 REPLACES DD FORM 1473, 1 JAN 64, WHICH IS OBSOLETE FOR ARMY USE.

Unclassified

Security Classification

14 KEY WORDS	LINK A		LINK B		LINK C	
	ROLE	WT	ROLE	WT	ROLE	WT
Deformation	8		9		9	
Tents	9		9		9	
Cylindrical	0		0			
Inflated	0		0			
Single-wall	0		0			
Wind	10					
Pressure	10					
Analysis			8		8	
Numerical Analysis			10		8	
Stresses					9	
Shape					9	
Aerodynamic Configurations					9	
Anchors (Structural)					9	
Force					9	